Supplemental material to "Rydberg Atom-Enabled Spectroscopy of Polar Molecules via Förster Resonance Energy Transfer"

Sabrina Patsch,[†] Martin Zeppenfeld,[‡] and Christiane P. Koch[*,†]

†*Dahlem Center for Complex Quantum Systems and Fachbereich Physik, Freie Universität Berlin, Arnimallee 14, 14195 Berlin, Germany*

‡*Max-Planck-Institut für Quantenoptik, Hans-Kopfermann-Straße 1, 85748 Garching, Germany*

E-mail: christiane.koch@fu-berlin.de

Details of the molecular model

We consider FRET between Rydberg atoms and the inversion vibrational mode of ammonia. The latter can be modelled as a symmetric top rotor and its states can be described in terms of the symmetric top eigenstates $|JKM\rangle$. We use the standard notation with angular momentum quantum number J and projections onto the molecular symmetry axis K and onto the space-fixed Z-axis M.[1] The inversion mode, with level splitting equal to 23.694 GHz, then couples the $+K$ and $-K$ states. The rotational subspace with $J = K = 0$ does not possess an inversion mode and thus does not contribute to the FRET signal. For $J = |K| = 1$, the transition matrix elements between states within the upper and lower inversion manifold are of the order of 0.5 D. At a given temperature, the occupation of the rotational states depends on J and K and is given by $f_{JK}(T) = g/\mathcal{N} e^{-\frac{E_{JK}}{k_B T}}$ with T the temperature, $\mathcal{N}$ a normalization factor, and g the statistical weight of the state. The statistical weight is $g = 2(2J+1)$ except for $K = 3m$ with $m \geq 1$ where $g = 4(2J+1)$ due to the three-fold symmetry of ammonia.[2]

Details of the model for the Rydberg atom

We consider the single valence electron of a rubidium-85 atom. We use the known quantum defects[3–5] up to $\ell = 7$ to describe the energy levels at zero electric field in the spherical basis $|n\ell m\rangle$. Except for fixing the quantum defect as $\delta_{n\ell} = \delta_{n\ell,j=\ell+1/2}$, our model negects spin-orbit coupling in the rubidium atom. A full account of spin-orbit orbit coupling will slightly change our predictions, depending on the experimental resolution. In particular, energy level shifts and matrix elements between energy levels as a function of electric field will be somewhat different which may affect precise lineshapes and line positions.

We evaluate the influence of the static electric field described by the Hamiltonian $\hat{V}_{\text{ryd}}^{\text{DC}} = \hat{z} F_{\text{DC}}$ by computing the matrix elements of the z-operator. The angular part is calculated analytically while the radial part is calculated numerically using Numerov's method taking the modified potential of the Rydberg atom into account.[6] Afterwards, we diagonalize the Hamiltonian numerically to obtain the eigenvalues of the Rydberg atom in the DC dressed basis. To improve accuracy, we take all states with $n = 44 \pm 2$ into account in the diagonalization, not only the two manifolds $45d$ and $46p$. Afterwards, all states but $45d$ and $46p$ are removed from the set to speed up numerical calculations. The matrix elements between $45d$ and $46p$ are calculated equivalently as described above and take values up to 3000 D.

Validity of the model

Our model relies on two basic assumptions — the translational motion can be treated classically, and the state of the Rydberg atom faithfully represents the Förster resonant energy transfer with the polar molecule. In the following, we assess the validity of these assumptions.

(1) The approximation of a classical, straight trajectory only remains valid as long as the kinetic energy E_{kin} is much larger than the interaction strength V_{dd} between the particles. The latter depends on the distance between the two particles. A suitable estimate for this

distance is given by the impact parameter at which the population exchange between the particles is maximal and which we term critical impact parameter. Its scaling with the relative velocity can be derived as follows. For the particles to exchange population, the phase accumulated by the particles, $\Phi = V_{\mathrm{dd}}T$, needs to be of the order of one, $\Phi \sim 1$. The interaction scales as $V_{\mathrm{dd}} \sim r^{-3}$ (cf. Eq. (2) in the main text) and the time during which the two particles interact significantly can be approximated as $T \sim r/v$. Combining the equations and solving for the critical impact parameter $r = b^*$ results in the scaling

$$b^* = \frac{c}{\sqrt{v}}. \tag{1}$$

The proportionality constant c is obtained from the numerical simulations by multiplying the impact parameter at which the exchange probability is maximal with the square-root of the velocity. We find the constant to be $c = 1.66 \cdot 10^{-6}\,\mathrm{m}\sqrt{\frac{\mathrm{m}}{\mathrm{s}}}$. For $v = 0.1\,\mathrm{m/s}$, the critical impact parameter amounts to $b^* = 5\,\mu\mathrm{m}$. We find that the condition for the energy scale separation is fulfilled with the kinetic energy, $E_{\mathrm{kin}} = 180\,\mathrm{kHz}$, being three orders of magnitude larger than the interaction energy, $V_{\mathrm{dd}} = 1.6\,\mathrm{kHz}$. Only at relative velocities below $8 \cdot 10^{-6}\,\mathrm{m/s}$ will the two energies become equal (0.001 Hz).

(2) Due to their interaction with the Rydberg atom, some molecules will be deflected from a straight trajectory. This deflection is neglected in our model. We estimate the percentage of trajectories which are subject to deflection as follows: Deflection occurs if the potential energy is of the same order of magnitude as the kinetic energy. For a given velocity, equating kinetic and potential energy and solving for the distance results in the impact parameter b_d at which deflection occurs,

$$b_d = \left(\frac{d_{\mathrm{mol}} d_{\mathrm{ryd}}}{2\pi\epsilon_0 \mu v^2}\right)^{\frac{1}{3}}. \tag{2}$$

With $d_{\mathrm{mol}} \approx 0.5\,\mathrm{D}$, $d_{\mathrm{ryd}} \approx 3000\,\mathrm{D}$ and μ the reduced mass, this yields, for the lowest velocity considered in the main text, $v = 1\,\mathrm{m/s}$, $b_d \approx 230\,\mathrm{nm}$. Assuming the scattering centre to be a hard sphere, the corresponding cross section would be $\sigma_{\mathrm{sphere}} = \pi b_d^2 = 1.7 \cdot 10^{-9}\,\mathrm{cm}^2$. This is more than one hundred times smaller than the peak cross section determined numerically (about $200 \cdot 10^{-9}\,\mathrm{cm}^2$, cf. Fig. 2(b) in the main text). Therefore, less than 1% of all trajectories describe scattering events in which the Rydberg atom and molecule come close enough to each other for significant deflection to occur. At higher velocities, this fraction is even smaller.

(3) Furthermore, assuming a classical trajectory also relies on the de Broglie wavelength ($\lambda_B = h/\mu v$ with reduced mass μ) being much smaller than the distance between the particles. For $v = 0.1\,\mathrm{m/s}$, the critical impact parameter, $b^* = 5\,\mu\mathrm{m}$, is one order of magnitude larger than the de Broglie wavelength, $\lambda_B = 0.3\,\mu\mathrm{m}$. Only at relative velocities below $3 \cdot 10^{-4}\,\mathrm{m/s}$ will the de Broglie wavelength become equal to the critical impact parameter ($100\,\mu\mathrm{m}$).

(4) The duration of the experiment is limited by the lifetime of the Rydberg atom. For the Rydberg states considered in this work and at room temperature, the lifetime is mainly limited by decay processes induced by blackbody radiation and is around $75\,\mu\mathrm{s}$ (calculated using the *ARC* library[7]). The interaction time which is necessary for the particles

to exchange a significant amount of population is easiest approximated when assuming a quasi-stationary setup in which the beginning and end of the experiment is defined by the excitation of the atom to the Rydberg regime and its ionisation. Using the critical impact parameter as derived above, the interaction time can be approximated as $T = \frac{2b^*}{v}$. Inserting Eq. (1), solving for v and inserting as interaction time the lifetime of the Rydberg atom, we obtain the critical velocity of 0.1 m/s. As a result, the model is mainly limited by the lifetime of the Rydberg atom and remains valid approximately until relative velocities of 0.1 m/s.

(5) The state of the Rydberg atom represents the Förster resonant energy transfer faithfully, provided the interaction is not too strong. For example, if the molecule gets very close to the Rydberg atom and possibly even enters the Rydberg orbit, the interaction becomes so strong that both atom and molecule undergo many transitions, akin to Rabi cycling. On average, every state of the considered Rydberg subspace is populated with equal probability. In terms of the cross sections, this merely increases the noise level somewhat.

Approximation of necessary molecular densities

In the following, we elaborate on the estimation of the molecular density which is required to detect the molecules via their interaction with Rydberg atoms. First, the effective volume that a Rydberg atom probes during a given time T can be approximated as $V = Tv\sigma$. When inserting the peak values of the cross section from Fig. 2(b-d), for instance $\sigma \sim 2 \cdot 10^{-7}\,\mathrm{cm}^2$ at $v = 1\,\mathrm{m/s}$, and assuming a maximal interaction time of $T = 100\,\mu\mathrm{s}$ (limited by the finite lifetime of the Rydberg state), we obtain the value of $V = 2 \cdot 10^{-9}\,\mathrm{cm}^3$ as given in the main paper. This value is independent of v as σ scales as $1/v$, cf. Eq. (6). Second, at a molecular density ϱ, the Rydberg atom interacts on average with $N = \varrho V$ molecules. At a molecular density of $5 \cdot 10^8\,\mathrm{cm}^{-3}$, the Rydberg atom then interacts on average with exactly one molecule and the signal is saturated. At higher densities, our approximation of a dilute medium breaks down. At lower densities, the signal reduces accordingly. When trapping, for instance, a single molecule in an optical tweezer with an estimated volume of $10^{-8}\,\mathrm{cm}^3$, this corresponds to a density of $10^8\,\mathrm{cm}^{-3}$ and 20% of the saturated signal is achievable.

In a real experiment, these values have to be compared to the measured background. In the experiment,[8] the background is dominated by blackbody radiation which causes the Rydberg atom to change its state even if no molecules are present. Due to this effect, about 2% of the Rydberg atoms were found in the excited state.[8] Then the FRET signal and the background are of the same order of magnitude at a molecular density of $10^7\,\mathrm{cm}^{-3}$. This value can be further reduced by a few orders of magnitude: at $10^5\,\mathrm{cm}^{-3}$, the FRET signal is hundred times smaller than the background but observing a change of 1% in in the background transfer rate seems realistic. Of course, going to a setup with shielding of room temperature blackbody radiation, i.e., a cryogenic setup, would reduce the lower bound on the density for which molecules can be detected even further.

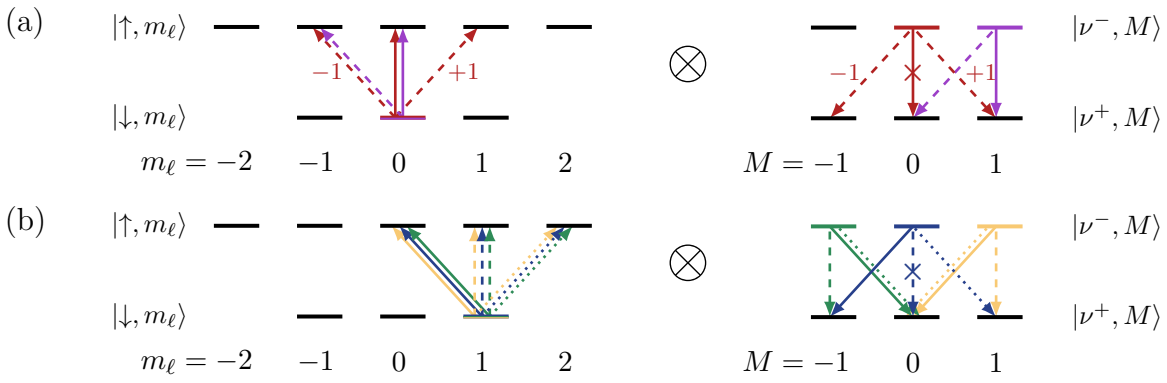

Figure S1: Dominant transition in the combined system of Rydberg atom (left) and molecule (right) as shown in Fig. 2. (a) shows transitions for initial states with $m_\ell = 0$. Solid lines indicate the resonance $|\downarrow, m_\ell = 0; \nu^-, M\rangle \leftrightarrow |\uparrow, m_\ell = 0; \nu^+, M'\rangle$ which occurs at 92 V/m, dashed lines indicate the resonance $|\downarrow, m_\ell = 0; \nu^-, M\rangle \leftrightarrow |\uparrow, m_\ell = \pm 1; \nu^+, M'\rangle$ which occurs at 107 V/m. (b) shows transitions for initial states with $m_\ell = 1$. Solid lines indicate the resonance $|\downarrow, m_\ell = 1; \nu^-, M\rangle \leftrightarrow |\uparrow, m_\ell = 0; \nu^+, M'\rangle$ which occurs at 77 V/m, dashed lines indicate the resonance $|\downarrow, m_\ell = 1; \nu^-, M\rangle \leftrightarrow |\uparrow, m_\ell = 1; \nu^+, M'\rangle$ which occurs at 85 V/m, dotted lines indicate the resonance $|\downarrow, m_\ell = 1; \nu^-, M\rangle \leftrightarrow |\uparrow, m_\ell = 2; \nu^+, M'\rangle$ which occurs at 149 V/m. The line colours of the arrows indicate the initial state using the same colour code as in Fig. 2(b-d).

Detailed analysis of the peak structure in the electric field-controlled cross section of Fig. 2

Figure 2 shows an intricate pattern of dips and peaks in the cross section as a function of the electric field. As discussed in the main text, the line shape can be traced back to the dominant transition occurring in the system. The possible kind of transitions, as discussed with the help of Fig. 3 in the main text, are summarised in Tab. 1. This, together with the location of the resonance allows one to determine the dominant transition occurring in the combined system of Rydberg atom and molecule. (1) The peak position of resonance as a function of electric field strength reveals which transition occurs in the Rydberg atom as shown in Fig. 2(a). This gives the value of Δm_ℓ. (2) The line shape reveals whether a criss-cross or flip-flop transition occurs as shown in Tab. 1. (3) Combining both, the value of ΔM can be concluded. We conduct this procedure in the following for all lines shown in Fig. 2.

Table 1: Overview of the types of transitions caused by dipole-dipole interaction.

name	selection rule	line shape
criss-cross	$\Delta m_\ell = \quad \Delta M = \pm 1$	peak
linear flip-flop	$\Delta m_\ell = \quad \Delta M = 0$	dip
diagonal flip-flop	$\Delta m_\ell = -\Delta M = \pm 1$	dip

In the main text, we have discussed as an example the initial state $|\downarrow, m_\ell = 0\rangle \otimes |\nu^-, M = 1\rangle$ (purple line in Fig. 2(b-d)). The dominant transitions are furthermore illustrated in Fig. S1(a). We found the peak at 107 V/m (corresponding to the resonance $|\downarrow, m_\ell = 0; \nu^-, M\rangle \leftrightarrow |\uparrow, m_\ell = \pm 1; \nu^+, M'\rangle$) being due to a criss-cross transition to $|\uparrow, m_\ell = -1\rangle \otimes |\nu^+, M = 0\rangle$ (purple dashed arrows in Fig. S1). The dip around 92 V/m ($|\downarrow, m_\ell = 0; \nu^-, M\rangle \leftrightarrow |\uparrow, m_\ell = 0; \nu^+, M'\rangle$), on the other hand, can be attributed to a linear flip-flop transition to $|\uparrow, m_\ell = 0\rangle \otimes |\nu^+, M = 1\rangle$ (purple solid arrows in Fig. S1).

The initial state $|\downarrow, m_\ell = 0\rangle \otimes |\nu^-, M = 0\rangle$ (red) shows a qualitatively similar behaviour as $|\downarrow, m_\ell = 0\rangle \otimes |\nu^-, M = 1\rangle$ (purple), since the Rydberg atom is initially in the same state. At 107 V/m, criss-cross transitions with both $\Delta m_\ell = \Delta M = \pm 1$ are allowed (as indicated next to the red dashed arrows in Fig. S1(a)). Moreover, the linear flip-flop transition to $|\uparrow, m_\ell = 0\rangle \otimes |\nu^+, M = 0\rangle$, suggested by the dip at 92 V/m ($|\downarrow, m_\ell = 0; \nu^-, M\rangle \leftrightarrow |\uparrow, m_\ell = 0; \nu^+, M'\rangle$), is forbidden by the molecular selection rule $M = 0 \not\leftrightarrow M' = 0$ (as indicated by the red solid arrows in Fig. S1(a)). Instead, the molecule performs transitions with $\Delta M = \pm 1$ leading to a dip in the electric field-controlled cross section.

The other three initial states correspond to the Rydberg atom being initially in $m_\ell = 1$ and thus relate to the resonances indicated by vertical blue lines in Fig. 2. The dominant transitions are illustrated in Fig. S1(b). We continue with the initial state $|\downarrow, m_\ell = 1\rangle \otimes |\nu^-, M = 0\rangle$ (blue). The cross section of this initial state shows a strong peak at the $|\downarrow, m_\ell = \pm 1; \nu^-, M\rangle \leftrightarrow |\uparrow, m_\ell = \pm 2; \nu^+, M'\rangle$ transition at 149 V/m. The line shape clearly indicates a criss-cross transition (i.e. $\Delta m_\ell = \Delta M = \pm 1$). The sign of the criss-cross transition can be deduced from the resonance itself which reveals that the Rydberg atom performs a transition from $46p, m_\ell = 1$ to $45d, m_\ell = 2$. Combining the two insights, we can deduce that the dominant transition occurs to the state $|\uparrow, m_\ell = 2\rangle \otimes |\nu^+, M = 1\rangle$ (dotted blue lines in Fig. S1(b)). The cross section also forms a peak around the resonance at 77 V/m ($|\downarrow, m_\ell = \pm 1; \nu^-, M\rangle \leftrightarrow |\uparrow, m_\ell = 0; \nu^+, M'\rangle$). Using similar arguments, the dominant transition is also a criss-cross transition to the state $|\uparrow, m_\ell = 0\rangle \otimes |\nu^+, M = -1\rangle$ (solid blue lines in Fig. S1(b)). Around the resonance at 85 V/m ($|\downarrow, m_\ell = \pm 1; \nu^-, M\rangle \leftrightarrow |\uparrow, m_\ell = \pm 1; \nu^+, M'\rangle$), the cross section forms a dip indicating a flip-flop transition. As the resonance indicates the Rydberg atom to perform a transition from $46p, m_\ell = 1$ to $45d, m_\ell = 1$, we can identify the linear flip-flop transition to $|\uparrow, m_\ell = 1\rangle \otimes |\nu^+, M = 0\rangle$ to be dominant (dashed blue lines in Fig. S1(b)). However, this transition is again forbidden by the molecular selection rule $M = 0 \not\leftrightarrow M' = 0$. Instead, the molecule performs transitions with $\Delta M = \pm 1$ which equally leads to a dip in the electric field-controlled cross section.

The initial state $|\downarrow, m_\ell = 1\rangle \otimes |\nu^-, M = -1\rangle$ (green) shows a qualitatively very similar behaviour to $|\downarrow, m_\ell = 1\rangle \otimes |\nu^-, M = 0\rangle$ (blue), since similar transitions are involved. The only qualitative difference between the two occurs at the resonance around 77 V/m ($|\downarrow, m_\ell = \pm 1; \nu^-, M\rangle \leftrightarrow |\uparrow, m_\ell = 0; \nu^+, M'\rangle$). The green line forms dip here while the blue one forms a peak. The green state therefore performs a diagonal flip-flop transition to $|\uparrow, m_\ell = 0\rangle \otimes |\nu^+, M = 0\rangle$ (solid green lines in Fig. S1(b)).

Finally, the state $|\downarrow, m_\ell = 1\rangle \otimes |\nu^-, M = 1\rangle$ (yellow) also shows a similar behaviour to $|\downarrow, m_\ell = 1\rangle \otimes |\nu^-, M = 0\rangle$ (blue), but deviates around the resonance at 149 V/m ($|\downarrow, m_\ell = \pm 1; \nu^-, M\rangle \leftrightarrow |\uparrow, m_\ell = \pm 2; \nu^+, M'\rangle$) as it shows a dip instead of a peak. Instead of a criss-cross, this state performs a diagonal flip-flop transition with $\Delta m_\ell = -\Delta M = 1$, driving the population to $|\uparrow, m_\ell = 2\rangle \otimes |\nu^+, M = 0\rangle$ (dotted yellow lines in Fig. S1(b)) and causing the strong dip in

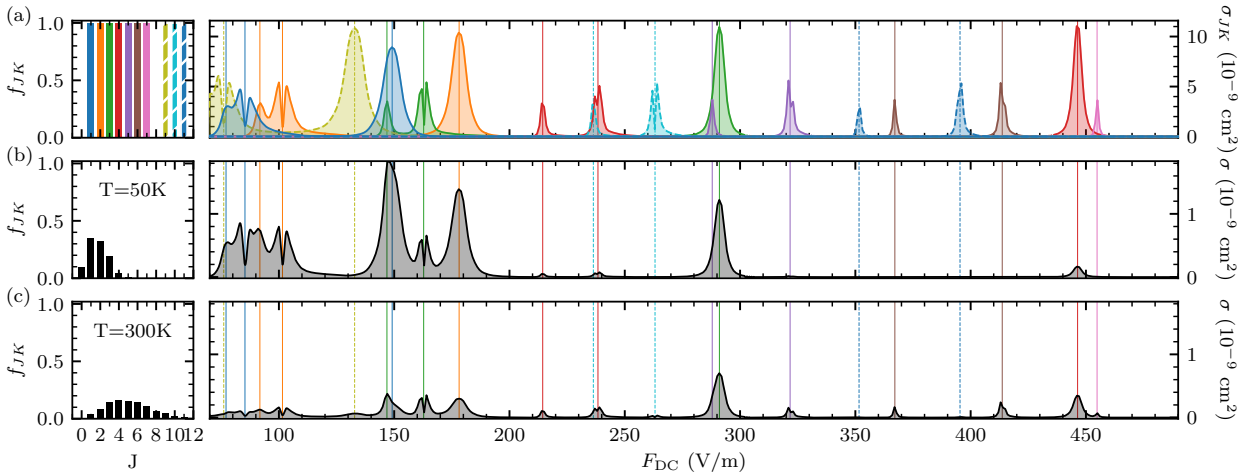

Figure S2: Like Fig. 4 but for $m_\ell = 1$: Rubidium Rydberg spectroscopy of ammonia with M-averaged cross sections shown on the right (for $v = 10\,\mathrm{m/s}$ and $m_\ell = 1$) and relative populations of the rotational states shown on the left for single rotational levels (a) and thermal ensembles (b,c) at rotational temperatures of 50 and 300 K, respectively. The vertical lines indicate resonances between the Rydberg transition and the inversion mode. Solid lines indicate $K = J$, dashed lines $K = J - 1$ (other molecular transitions are far off-resonant).

the spectrum.

It shall lastly be noted that cross sections do not completely vanish at resonance for flip-flop transitions (which form a dip) in the realistic model shown in Fig. 2, while in the simplified model of Fig. 3 they do. The reason is that for multi-level systems, the dynamics cannot be limited to a single transition. For instance, we have discussed that the initial state $|\downarrow, m_\ell = 1\rangle \otimes |\nu^-, M = 1\rangle$ (yellow state in Fig. 2) leads to a dip in the cross section at the $|\downarrow, m_\ell = \pm 1; \nu^-, M\rangle \leftrightarrow |\uparrow, m_\ell = \pm 2; \nu^+, M'\rangle$ transition at 149 V/m thus transferring population into $|\uparrow, m_\ell = 2\rangle \otimes |\nu^+, M = 0\rangle$. This state could further be transferred to $|\downarrow, m_\ell = 1\rangle \otimes |\nu^-, M = -1\rangle$ via a criss-cross transition. Thus, a fraction of the population is now in the state which we indicated by the green colour. In a second order process, this state can thus undergo a criss-cross transition leading to a peak at the considered $|\downarrow, m_\ell = \pm 1; \nu^-, M\rangle \leftrightarrow |\uparrow, m_\ell = \pm 2; \nu^+, M'\rangle$ transition which overlays with the initial dip created by the dominant flip-flip transition.

Molecules in an ensemble of rotational states for $m_\ell = 1$

We now present the dependence of the electric field-controlled cross section on the rotational quantum numbers J and K assuming the Rydberg atom to be initially in $46P, m_\ell = 1$. This is equivalent to the results presented in the section "Molecules in an ensemble of rotational states" of the main paper but changing m_ℓ from 0 to 1. The results are shown in Fig. S2 where three resonances appear for each rotational state $|J, K\rangle$, giving rise to a richer spectrum as compared to $m_\ell = 0$. It can be seen that, different from Fig. 4, several peaks overlap, such

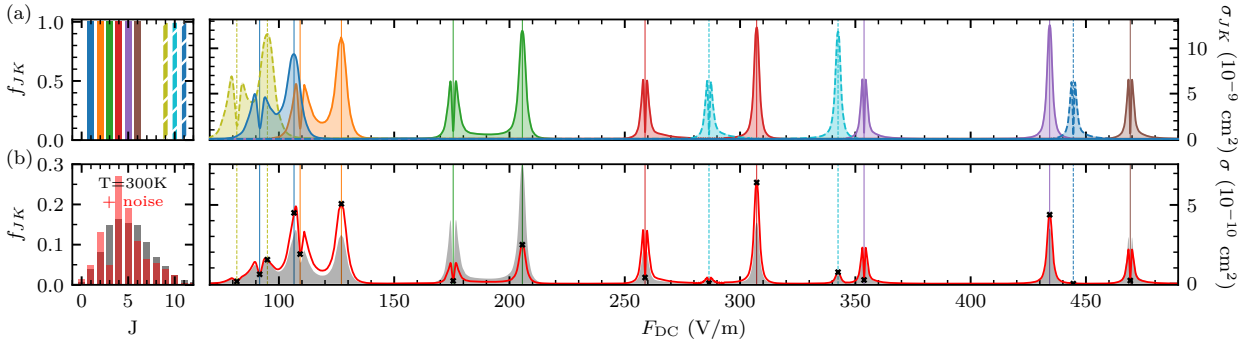

Figure S3: Similar to Fig. 4: Rubidium Rydberg spectroscopy of ammonia for $v = 10\,\mathrm{m/s}$ and $m_\ell = 0$. State-resolved cross sections are shown in (a), and (noisy) thermally averaged cross section in (b) panel. The red bar chart (b, left) and the red line (b, right) indicate the population distribution and corresponding cross sections when adding noise to a Boltzmann distribution with 300 K (black). The black crosses indicate the values used for fitting.

as the green ($J = K = 3$) and the purple ($J = K = 5$) one around 290 V/m. However, this does not hamper the fitting procedure. Each rotational sublevel gives rise to as least one peak which is sufficiently isolated from the others in order to determine its contribution to the cross section. For instance, even the $J = K = 1$ state (blue) can be clearly identified at 50 K by its characteristic double-peak structure close to 85 V/m in Fig. S2(b).

Fitting the relative populations from measured cross sections

Measuring the electric field-controlled cross section in an experiment allows for inferring the relative populations of rotational states. In the following, we sketch an example. First, we generate a noisy Boltzmann distribution which simulates an unknown distribution of rotational states in an experiment. We start from a Boltzmann distribution at 300 K (gray shade in left-hand panel of Fig. S3(b)) and add noise (red shade) by multiplying each component with a random number between 0 and 2, where a factor between 0 and 1 entails reduction and a factor between 1 and 2 increase of the corresponding component. We then re-normalise the distribution. When averaging the cross sections of single rotational levels (cf. Fig. S3(a)) accordingly, we obtain the signal shown in Fig. S3(b, red line). This curve will serve as the unknown signal acquired in an experiment and will be the starting point for the fitting procedure. Note that we did not add any further disturbance to the signal to simulate experimental noise. In particular, we did not alter the peak positions or their shape but kept them as given in Fig. S3(a). We expect the theoretical prediction to be very accurate, since the theoretical model of the Rydberg atom and the rotation and inversion mode of the molecule are very well known.

We test two different strategies for acquiring the composition of rotational states by fitting the theoretical data from Fig. S3(a) to our test signal from Fig. S3(b, red). First, we use the full information on the state-dependent cross sections $\sigma_{JK}(F_{\mathrm{DC}})$ as shown in Fig. S3(a)

which have a very high resolution. The averaged cross section $\sigma(F_{\mathrm{DC}})$ can be written as

$$\sigma(F_{\mathrm{DC}}) = \sum_{JK} c_{JK}\, \sigma_{JK}(F_{\mathrm{DC}}) \tag{3}$$

with $\sum_{JK} c_{JK} = 1$. We will treat the c_{JK} as fitting parameters which directly reflect the relative population of rotational states. Due to the resonance conditions, only 9 fitting parameters are left: c_{11} to c_{66} and c_{98} to $c_{11\,10}$. We perform the fit using the *optimize* package of *scipy* with guess parameters $c_{JK} = 1$. The guess signal is therefore identical to the sum on the peaks in Fig. S3(a). We find that the fit recovers the input parameters exactly and the fitted curve lies exactly on top of the red line in Fig. S3(b).

To test the applicability of the fitting procedure to real experimental data, we reduce the resolution of the signal. Namely, we only consider data points which are located directly at the resonances as indicated by the black crosses in Fig. S3(b), thus reducing the number of data points to 16. Note that the signal is very low at some resonances because the line forms a dip around them. We repeat the fitting procedure with this decreased resolution and find the correct input parameters with a relative error of 10^{-16}. Note that, when dealing with very small signals in a real experimental setting, it might be beneficial to measure the cross sections slightly next to the resonance. This increases the signal-to-noise ratio when detecting cross sections which form a dip at the resonance.

This example demonstrates that the relative populations of rotational states can be inferred with a very high resolution from a given input signal. Of course, the error of the fitting procedure will ultimately be given by the error bars of the experiment.

References

(1) Kroto, H. W. *Molecular Rotation Spectra*; John Wiley and Sons Ltd.: New York, 1975.

(2) Townes, C. H.; Schawlow, A. L. *Microwave Spectroscopy*; Dover Publications, Inc.: New York, 1975.

(3) Meschede, D. Centimeter-wave spectroscopy of highly excited rubidium atoms. *Journal of the Optical Society of America B* **1987**, *4*, 413–419.

(4) Han, J.; Jamil, Y.; Norum, D. V. L.; Tanner, P. J.; Gallagher, T. F. Rb nf quantum defects from millimeter-wave spectroscopy of cold ^{85}Rb Rydberg atoms. *Physical Review A* **2006**, *74*, 054502.

(5) Nussenzveig, P. Mesures de champs au niveau du photon par interférométrie atomique. Ph.D. thesis, Université Pierre et Marie Curie - Paris VI, France, 1994.

(6) Gallagher, T. F. *Rydberg atoms*; Cambridge Monographs on Atomic, Molecular, and Chemical Physics; Cambridge University Press: Cambridge, 1994.

(7) Šibalić, N.; Pritchard, J. D.; Adams, C. S.; Weatherill, K. J. ARC: An open-source library for calculating properties of alkali Rydberg atoms. *Computer Physics Communications* **2017**, *220*, 319–331.

(8) Jarisch, F.; Zeppenfeld, M. State resolved investigation of Förster resonant energy transfer in collisions between polar molecules and Rydberg atoms. *New Journal of Physics* **2018**, *20*, 113044.